Supporting Information

for

Nucleation of Biomimetic Hydroxyapatite Nanoparticles on the Surface of I-type Collagen: Molecular Dynamics Investigations

Zhiyu Xue[a], Mingli Yang[b,c] and Dingguo Xu[a,b]*

[a]*MOE Key Laboratory of Green Chemistry and Technology, College of Chemistry, Sichuan University, Chengdu, Sichuan, P. R. China*

[b]*Genome Research Center of Biomaterial, Sichuan University, Chengdu, Sichuan 610064, P. R. China*

[c]*Institute of Atomic and Molecular Physics, MOE Key Laboratory of High Energy Density Physics and Technology, Sichuan University, Chengdu, Sichuan, 610065, P. R. China*

* To whom correspondence should be addressed: dgxu@scu.edu.cn Tel: 86-28-85406156

Contents

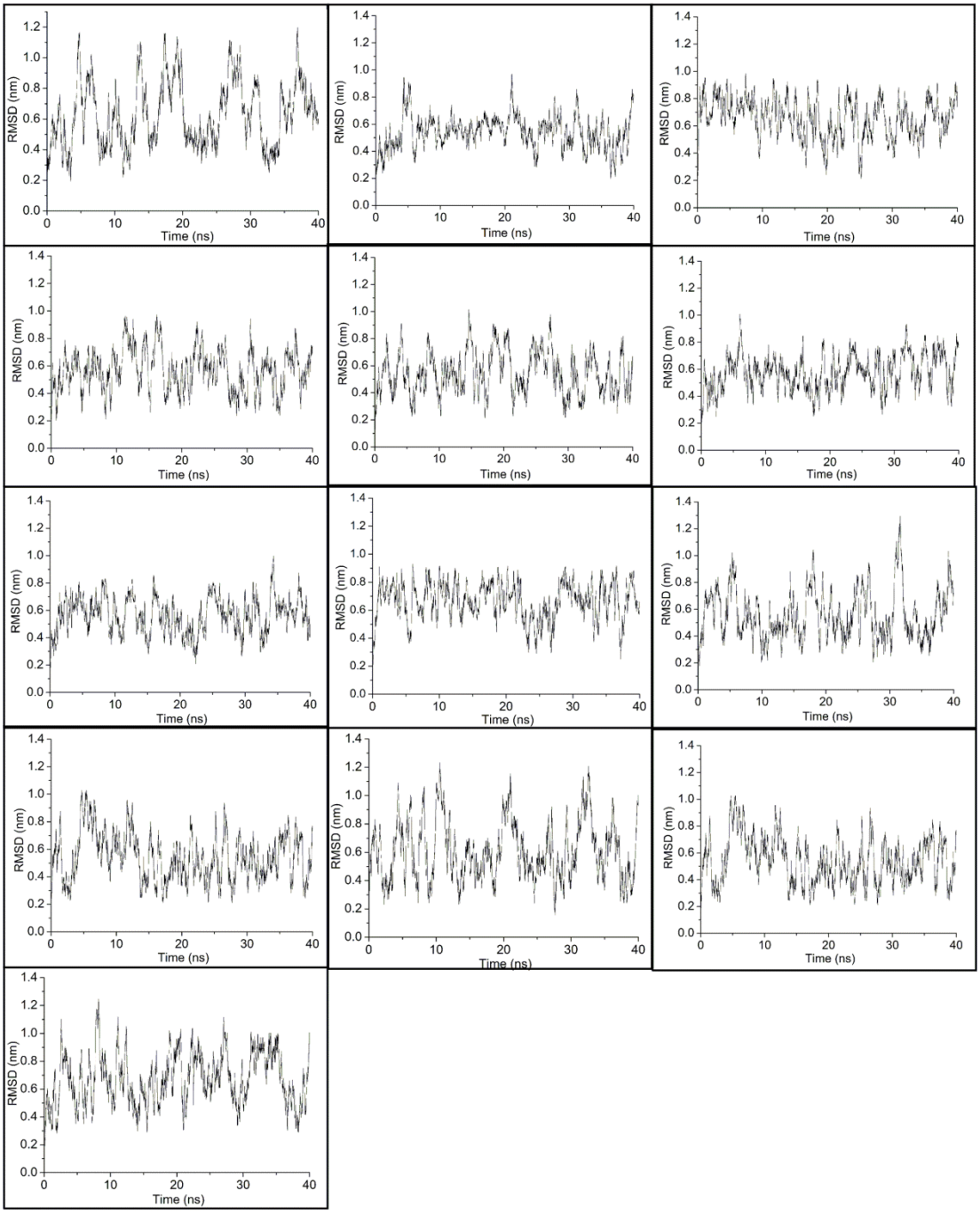

Figure S1. The root mean square deviation of backbone atoms of all thirteen collagen models throughout 40 ns MD simulation.

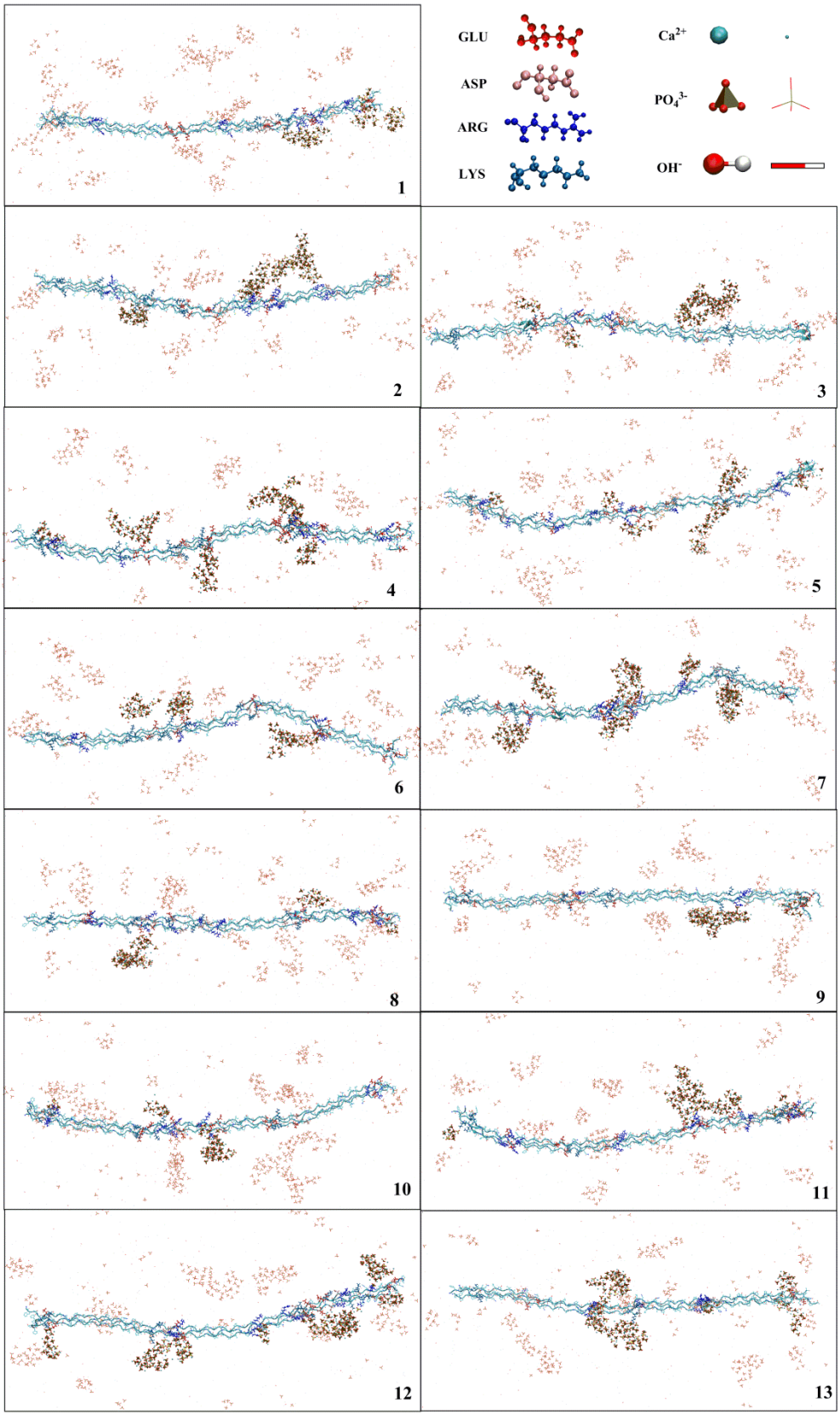

Figure S2. The overview of Ca-P cluster formation for all thirteen collagen segments after 10 ns MD simulation.

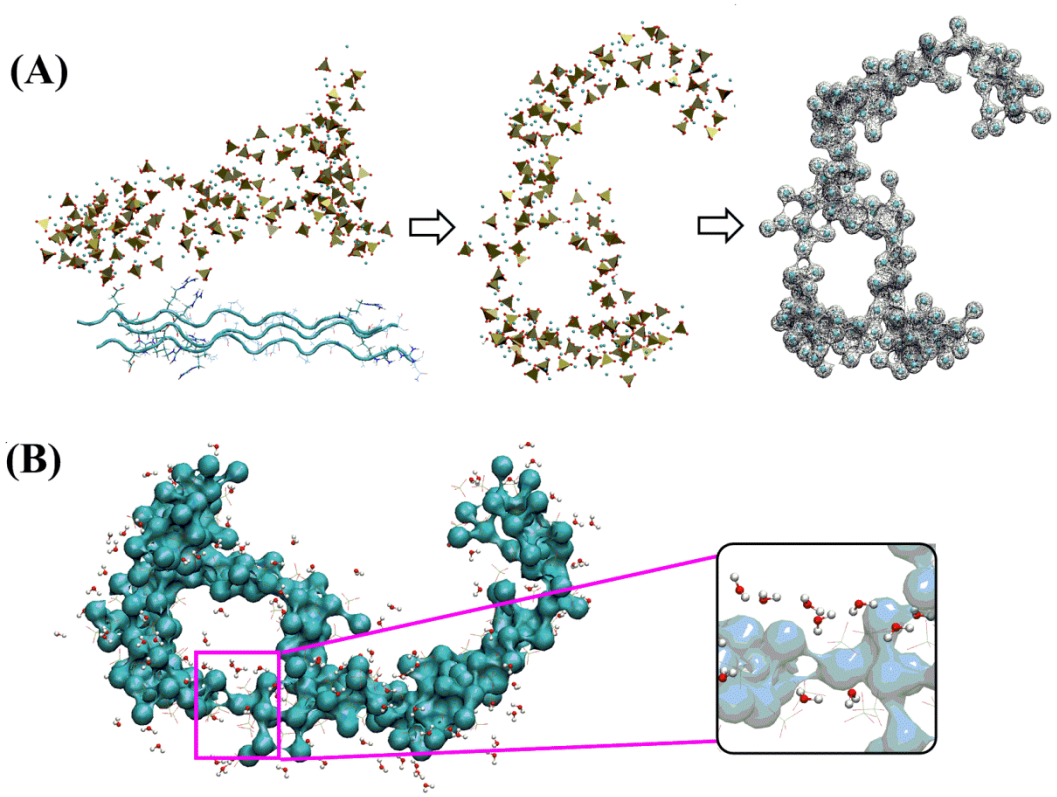

Figure S3. (A) One typical cluster ($Ca_{182}(PO_4)_{127}(OH)_9$) formed on the second collagen surface extracted from the last frame of MD trajectories. (B) The water distribution around the cluster with distance of 5 Å.

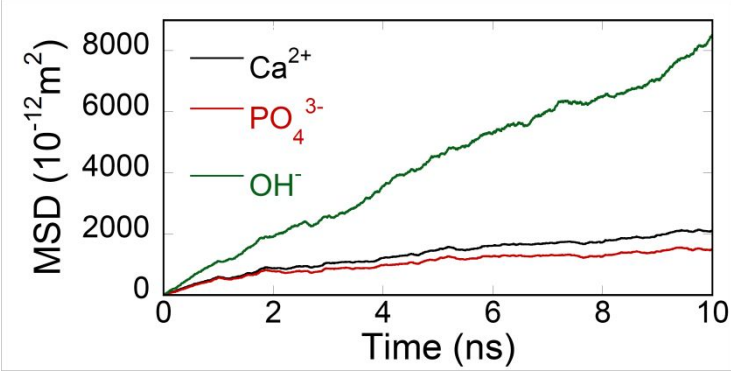

Figure S4. Mean square displacement (MSD) values for ions of Ca^{2+}, PO_4^{3-} and OH^- along the simulation time.

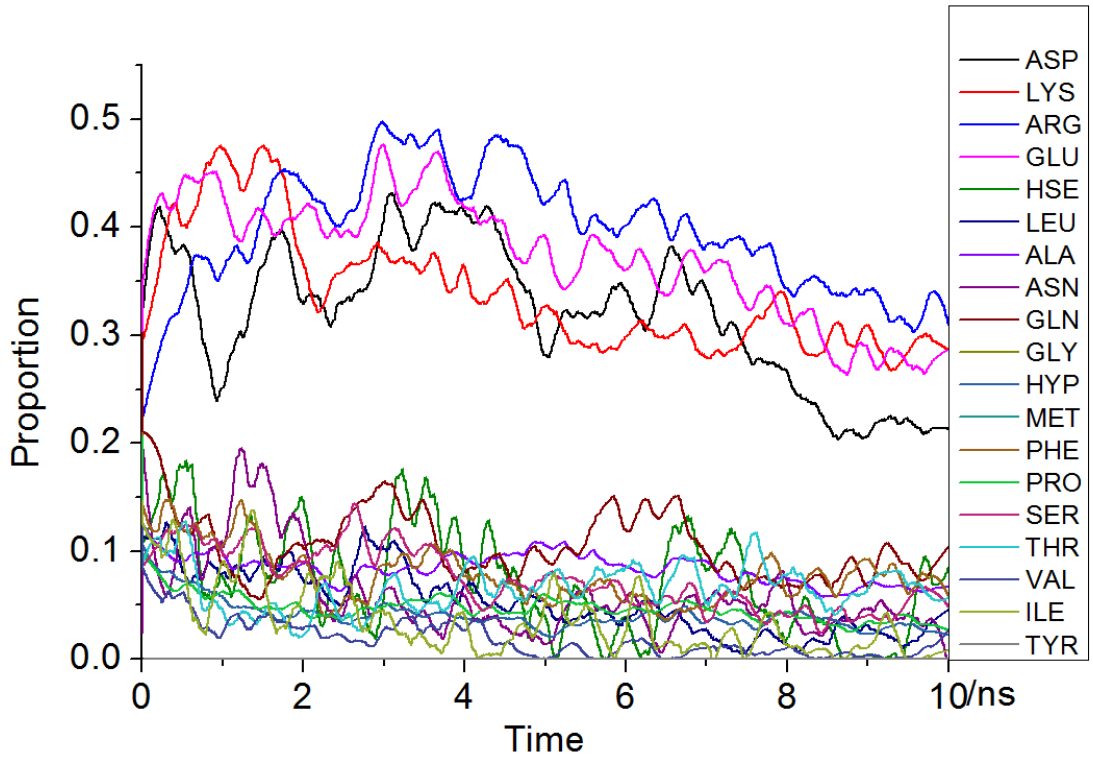

Figure S5. The cluster occurrence rate of the nucleation site containing different amino acids.

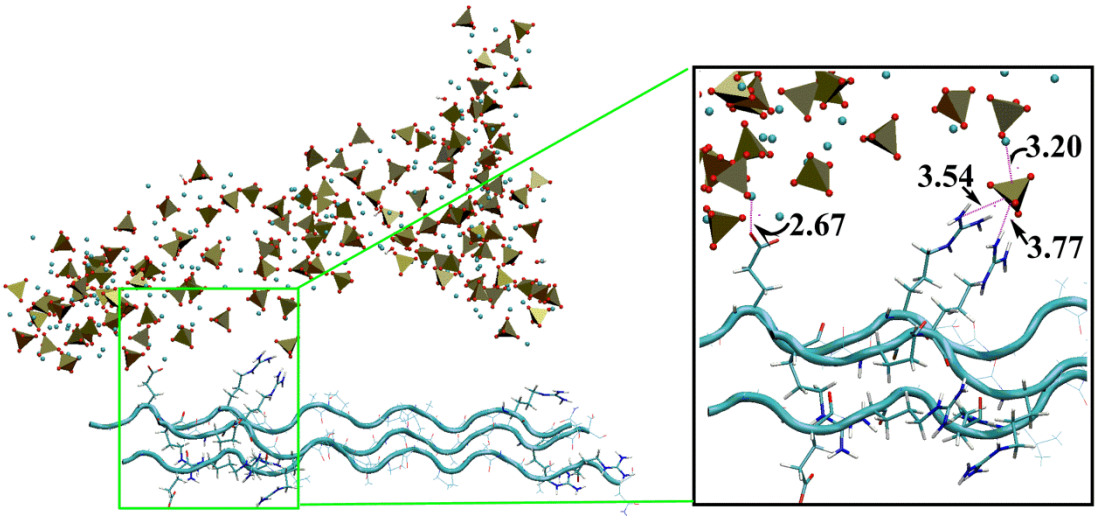

Figure S6. The detailed interaction patterns between the protein and one of clusters extracted from the second collagen segment, in which the cluster has the stoichiometry of $Ca_{182}(PO_4)_{127}(OH)_9$.

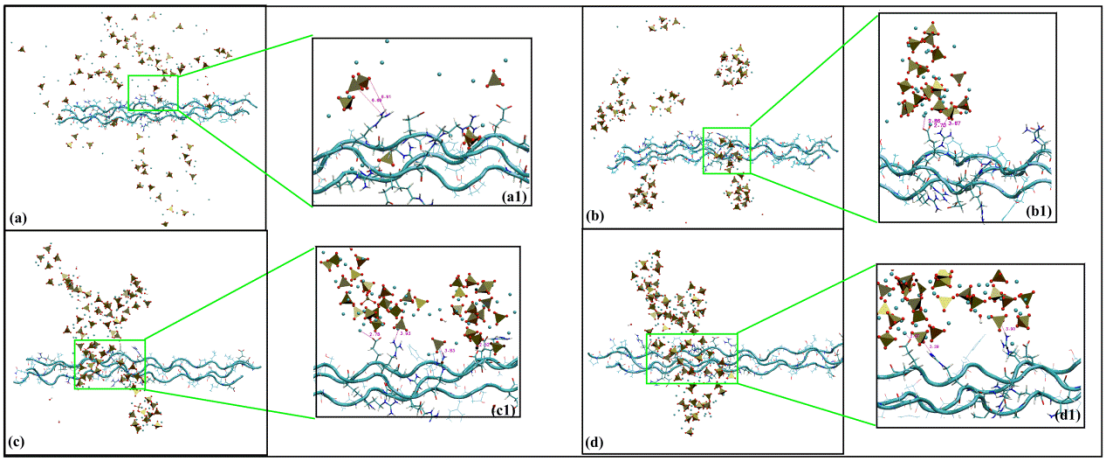

Figure S7. The evolution of one example cluster ($Ca_{108}(PO_4)_{72}(OH)_{10}$) in the 7th collagen segment extracted from the trajectory along the simulation time course (0ns,2ns,4ns,10ns). For detailed view, zoom-in presentations are given in the insert.

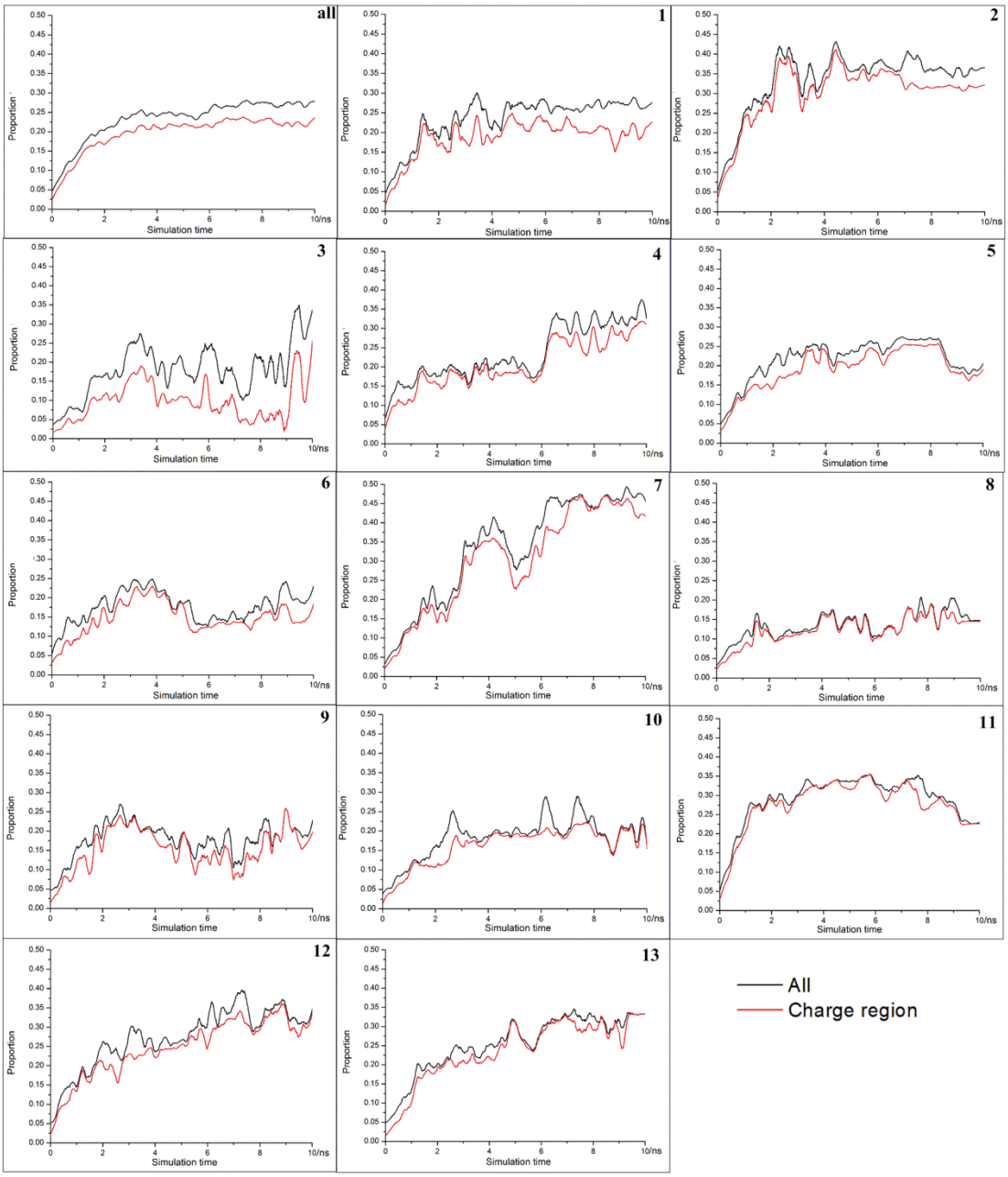

Figure S8. The probability of the nucleation on the collagen protein surface during the 10 ns simulation. In particular, the black curve denotes the possibility of calcium and phosphate ions occurring on the collagen surface, while the red color means the occurrence rate of clusters around the regions including charged residue.

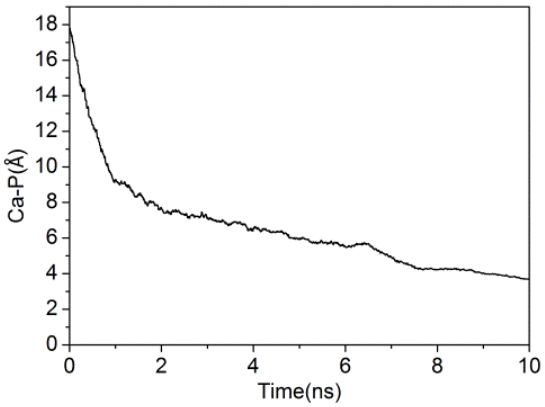

Figure S9. The evolution of distance between Ca and P atoms in the clusters close the collagen surface.

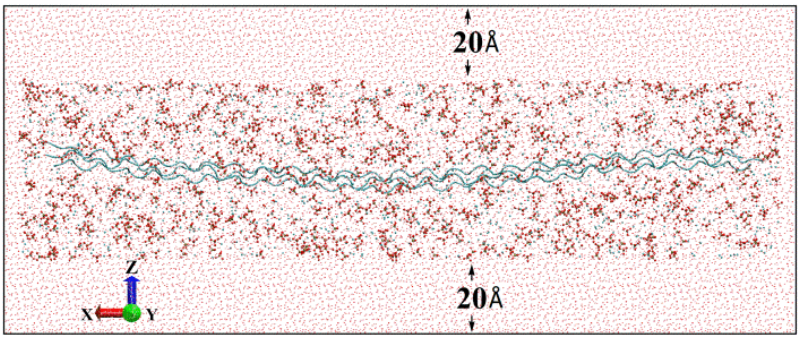

Figure S10. The initial state of collagen model, for which the Z direction is elongated by the 40 angstroms.

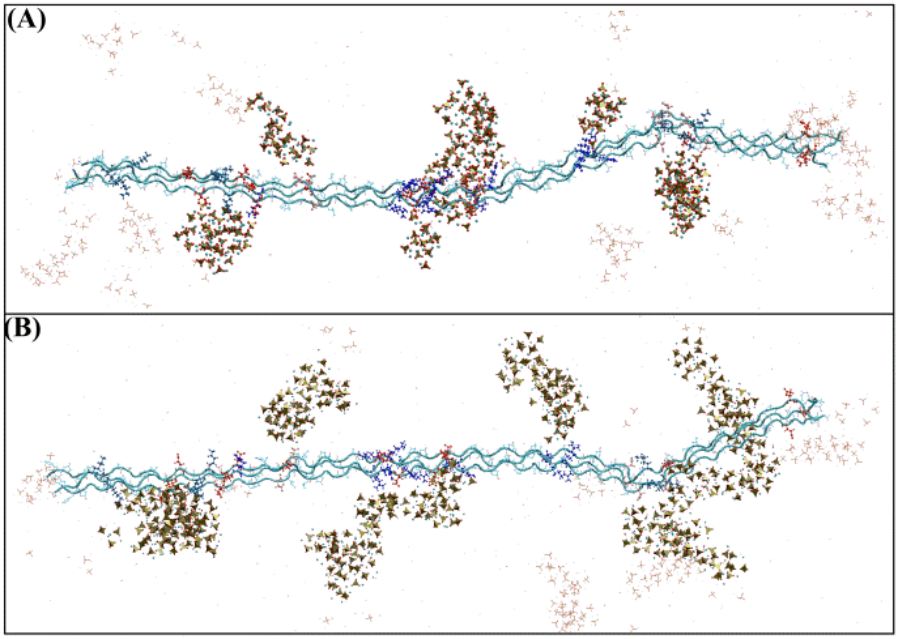

Figure S11. (A) The 7th segment of collagen model with box size 290 Å × 80 Å × 90 Å; (B) The 7th segment of collagen model with box size 290 Å × 80 Å × 130 Å

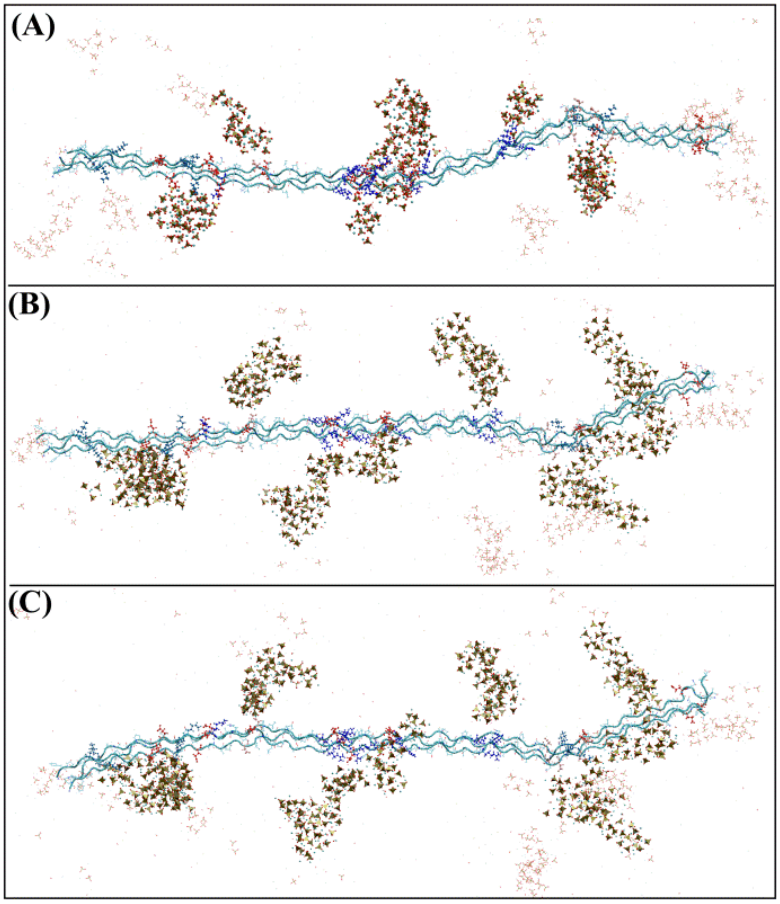

Figure S12. (A) The nucleation of the 7th segment of collagen model after 10 ns with box size of 290 Å × 80 Å × 90 Å; (B) The nucleation of the 7th segment of collagen model after 10 ns with box size of 290 Å × 80 Å × 130 Å; (C) The nucleation of the 7th segment of collagen model after 15 ns with box size of 290 Å × 80 Å × 130 Å.

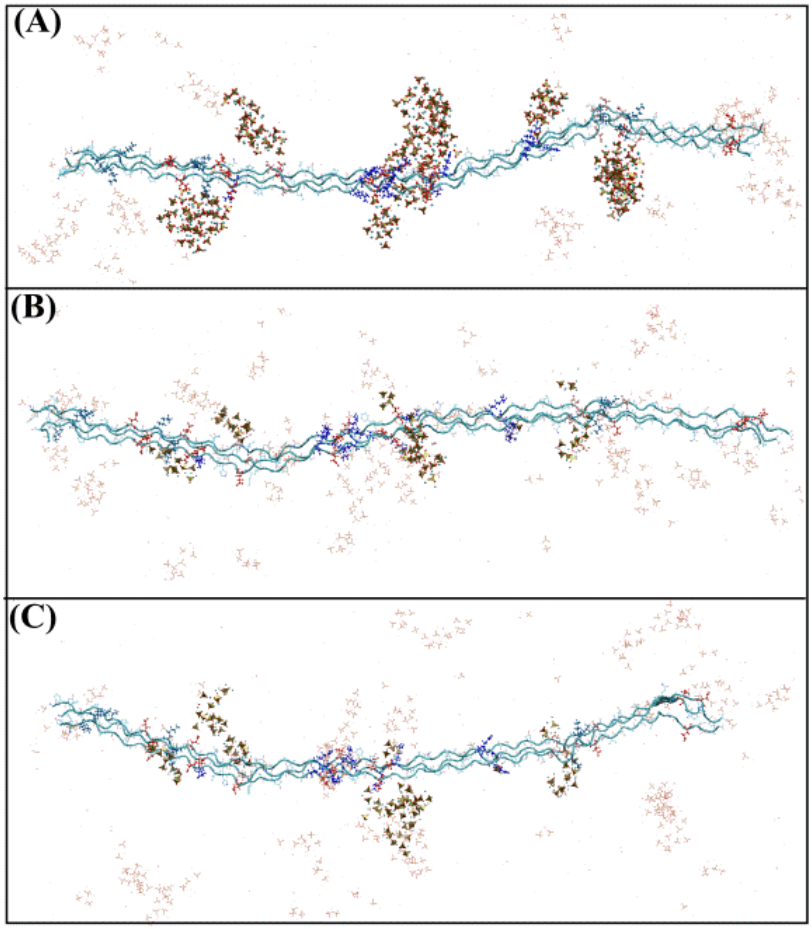

Figure S13. (A) The nucleation of the 7th segment of collagen model after 10 ns using INTERFACE force field; (B) The nucleation of the 7th segment of collagen model after 10 ns using the force field parameters from the reference of Yang et al., *Langmuir* 2010, 26, 9848-9859; (C) The nucleation of the 7th segment of collagen model using the same force field as (B), but 20 ns MD simulation.

Table S1. The summary of clusters formed in the 7th segment of collagen models after 2 ns MD simulation.

Number of Atom	Stoichiometry	Ca/P	Ponser's Cluster
110	$Ca_{25}(PO_4)_{17}$	1.471	Y
108	$Ca_{23}(PO_4)_{17}$	1.353	N
105	$Ca_{25}(PO_4)_{16}$	1.562	Y
102	$Ca_{23}(PO_4)_{15}(OH)_2$	1.533	Y
99	$Ca_{20}(PO_4)_{15}(OH)_2$	1.333	N
90	$Ca_{20}(PO_4)_{14}$	1.429	Y
90	$Ca_{18}(PO_4)_{14}(OH)$	1.286	N
72	$Ca_{17}(PO_4)_{11}$	1.545	Y
67	$Ca_{12}(PO_4)_{11}$	1.091	N
55	$Ca_{10}(PO_4)_9$	1.111	N
52	$Ca_{12}(PO_4)_8$	1.5	Y
48	$Ca_9(PO_4)_7(OH)_2$	1.286	N
45	$Ca_{10}(PO_4)_7$	1.429	Y

References

23. Liu, T.; Ding, X. B.; Lai, D. Z.; Chen, Y. W.; Zhang, R. D.; Chen, J. Y.; Feng, X. X.; Chen, X. Y.; Yang, X. Y.; Zhao, R. B.; Chen, K.; Kong, X. D., Enhancing in Vitro Bioactivity and in Vivo Osteogenesis of Organic-Inorganic Nanofibrous Biocomposites with Novel Bioceramics. *J. Mat. Chem. B* **2014,** *2*, 6293-6305.

36. Niu, L. N.; Jee, S. E.; Jiao, K.; Tonggu, L.; Li, M.; Wang, L.; Yang, Y. D.; Bian, J. H.; Breschi, L.; Jang, S. S.; Chen, J. H.; Pashley, D. H.; Tay, F. R., Collagen Intrafibrillar Mineralization as a Result of the Balance between Osmotic Equilibrium and Electroneutrality. *Nat. Mater.* **2017,** *16*, 370-378.